

Simulations of the heating of the Galactic stellar disc

Jyrki Hänninen¹ and Chris Flynn^{1,2}

¹*Tuorla Observatory, Väisäläntie 20, FIN-21500, Piikkiö, Finland*

²*Centre for Astrophysics and Supercomputing, Swinburne University of Technology, Hawthorn, Australia*

27 August 2021

ABSTRACT

The velocity dispersion of nearby stars in the Galactic disc are well known to increase substantially with age; this is the so-called Age-Velocity relation, and is interpreted as a “heating” of the disc as a function of time. We have studied the heating of the Galactic stellar disc due to giant molecular clouds and halo black holes, via simulations of the orbits of tracer stars embedded in a patch of the local Galactic disc. We examine a range of masses and number densities of the giant molecular cloud and halo black hole perturbers. The heating of the stellar disc in the simulations is fit with a simple power law of the $\sigma \propto t^\alpha$ where σ is the velocity dispersion of the tracer stars as a function of time, t . We also fit this form to the best determinations of the increase in the velocity dispersion as a function of time as derived from stars in the solar neighbourhood for which ages can be reliably assigned. Observationally, α is found to lie in the range 0.3 to 0.6, i.e. it remains poorly constrained and its determination is probably still dominated by systematic errors. Better constrained observationally is the ratio of the velocity dispersions of the stars in the vertical z and horizontal x (i.e. toward the Galactic center) directions, being $\sigma_z/\sigma_x = 0.5 \pm 0.1$.

For the heating of the stellar disc due to giant molecular clouds (GMCs) we derive a heating $\sigma \propto t^{0.21}$, which differs somewhat from early (analytic) studies in which $\sigma \propto t^{0.25}$. This confirms the well known results that there are insufficient GMCs to heat the Galactic disc appropriately. A range of dark halo black hole scenarios are verified to heat the stellar disc as $\sigma \propto t^{0.5}$ (as expected from analytical studies), and give σ_z/σ_x in the range 0.5 to 0.6, which is consistent with observations. Black holes with a mass of $10^7 M_\odot$ are our favoured disc heaters, although they are only marginally consistent with observations. Simulations featuring a combination of giant molecular clouds and halo black holes can explain the observed heating of the stellar disc, but since other perturbing mechanisms, such as spiral arms, are yet to be included, we regard this solution as ad hoc.

Key words: Galaxy: kinematics and dynamics – (Galaxy:) solar neighbourhood – Galaxy: velocity dispersion – N-body simulations

1 INTRODUCTION

The random motions of stars near the Sun are well known to increase with stellar age, and this effect is known as the disc Age Velocity Relation (hereafter AVR). Broadly speaking, the total velocity dispersion of stars rises from $\approx 20 \text{ km s}^{-1}$ at the lowest measurable ages to $\approx 60\text{--}80 \text{ km s}^{-1}$ at an age of $\approx 10\text{--}12 \text{ Gyr}$. The “heating” of the orbits is initially rapid but levels off after some Gyr. The heating is not uniform in each of the three velocity components; the velocity dispersion rises to a higher value in the Galactic plane than in the vertical direction.

A number of mechanisms have been proposed to explain the AVR, in particular the gravitational perturbative effect

on stellar orbits by giant molecular clouds (GMCs) in the Galaxy’s gas layer (Spitzer & Schwarzschild 1951; Spitzer & Schwarzschild 1953), by spiral arms in the disc (Barbanis & Woltjer 1967), or by massive black holes in the Galactic dark halo (BHs) (Lacey & Ostriker 1985). Dramatic disc heating also takes place when satellite galaxies fall onto galactic discs (Quinn & al. 1993), and such events may well leave an abrupt feature in the AVR, but if the rain of such satellites is relatively gentle they might also heat discs smoothly (Velazquez & White 1999).

Spitzer and Schwarzschild (1951; 1953) first argued that the observed growth of the stellar velocity dispersion could be explained by encounters of disc stars with GMCs with masses of $M_{\text{GMC}} \sim 10^6 M_\odot$. The main difficulty with this

arXiv:astro-ph/0208426v1 23 Aug 2002

scenario is that the observed number of GMCs modify stellar orbits in a manner inconsistent with observations. Firstly, they are too few to reproduce the observed heating, and secondly, too much heating is produced in the vertical direction relative to the disc plane (Lacey 1984). However, GMCs do exist so they certainly provide a mechanism for redirecting orbits out of the Galactic plane, whatever is responsible for the heating. Heating due to transient spiral arms suffers the opposite problem that the amount of vertical heating is too low compared to observations (Carlberg 1987).

This naturally leads to the idea that the observed heating could be explained by the combined effect of the transient spiral arms and giant molecular clouds. In this model spiral density waves would act as main source of heating and GMCs would deflect the stellar orbits out of the Galactic plane, thus creating the required velocity dispersion in the vertical direction (Carlberg 1987). However, these calculations are rather complicated: e.g. the relative effectiveness of spiral and GMC heating has to be modelled with an empirical parameter. The rate at which spiral features heat a stellar disc depends on the potential's spatial pattern and on the time variability of the pattern. In principle, spatial structures of galaxies can be determined from photometry of real galaxies and temporal information about spiral structure can be obtained from numerical simulation and dynamical theory. In practice, however, we do not have adequate information about strengths, growth rates or duty cycles of spiral features. So empirical parametrization has so far been the only possible approach (Jenkins & Binney 1990; Jenkins 1992).

Lacey and Ostriker (1985) proposed that the Galactic dark halo might consist of massive black holes (BHs) which would heat the disc as they pass through it. The total heating produced by their proposed $2 \times 10^6 M_{\odot}$ black holes is consistent with observations, but the velocity ellipsoid was found to be quite round, which is inconsistent with observations. Furthermore, if the dark halos of dwarf spiral galaxies were dominated by similar BHs their discs would be easily destroyed (Friese & al. 1995). Finally, BHs passing through the disc might be expected to accrete and reveal themselves as high proper motion X-ray sources, and no such objects have been seen. It seems worth noting though that the central black hole in the Milky Way demonstrates that the accretion rate and emergent flux from a black hole of about the desired mass ($2.6 \times 10^6 M_{\odot}$) is far from well understood (Genzel 1998); the central black hole in the Milky Way is remarkably quiet in X-rays. Another way of detecting these putative black holes is by statistically studying large numbers of orbits of nearby stars; this may be possible with very accurate distances and kinematics which will become available for stars within some kiloparsecs from ESA's GAIA satellite.

In order to avoid problems related to the black hole scenario Carr and Lacey (1987) proposed dark clusters of less massive objects. The latest generation of cosmological simulations of galaxy formation do indeed show quite clumpy dark halos around Milky Way type spirals (Moore et al. 1999). The amount, size and distribution of these clumps is still very uncertain, mainly due to numerical resolution issues, but if they can survive in the inner regions of dark halos they may well be able to heat discs in a manner consistent with observations.

With this in mind we have embarked on a new study of disc heating simulations, starting with examining heating due to GMCs and BHs. The European Space Agency's Hipparcos satellite has provided a wealth of new data on the distances and kinematics of nearby stars, so that one can now construct very much improved measurements of ages and kinematics. The velocities of the stars are much improved through the excellent Hipparcos parallaxes, while the ages of stars can be much better estimated, particularly for stars near the disc main sequence turn-off, because of the greatly improved absolute magnitudes.

Ideally, one would like to carry out a self-consistent N-body simulation of an entire disc galaxy, with and without the perturbing influences due to GMCs/BHs etc, but this is not yet possible even with the fastest computers. The computation would involve both the stars (at approx $1 M_{\odot}$) and the perturbers (for a range of masses, 10^5 - $10^7 M_{\odot}$), implying some 10^{11} stars and thousands of GMCs to millions of BHs in the simulations. This is not yet feasible in an N-body simulation. In this paper we render the problem tractable by simulating the heating in a local patch of the Galactic disc consisting typically of few tens of thousands of (massless) tracer stars, embedded within a fixed Galactic background potential, through which massive perturbers move. By using a local simulation method we can resolve very well the effects of perturbers on nearby stellar orbits, for comparison with the locally obtained observations. A very similar method has been used by Fuchs et al. (1994) who studied disc heating due to GMCs and/or $5 \times 10^6 M_{\odot}$ black holes. We are able to broadly reproduce the results of their code in this area, but we also explore a larger range of scenarios.

From our simulations, we find that GMC heating is less effective than earlier thought and further that heating due to GMCs creates a flatter velocity ellipsoid than found in earlier studies. We find that BHs are not as effective in heating the disc as earlier thought. However, very massive halo black holes ($M_{BH} = 1 \times 10^7 M_{\odot}$) can heat the disc up to the observed amount, but the results of the heating rate and the ratio of the velocity dispersions are only marginally consistent with observations. A well selected combination of BHs and GMCs can give the observed heating in every component of the velocity dispersion within the observational error limits, but while interesting this solution is probably ad hoc, as the simulations do not yet model the effects of other perturbation sources, such as spiral waves. This will be examined in future work.

This paper is organised as follows. In section 2 we review pre- and post-Hipparcos work on the observational determination of the age-velocity relation (AVR) for the local disc. We find the AVR is much less well measured than has previously been assumed. Observational issues thus still fundamentally limit our ability to discriminate between disc heating mechanisms. In section 3 we describe briefly our simulation method and numerical accuracy. In sections 4, 5, and 6 we demonstrate how massive perturbers (GMCs and halo BHs) heat up the stellar disc. We draw our conclusions in section 7.

2 OBSERVATIONS

The Hipparcos satellite measured parallaxes and space motions for a complete sky coverage of about 60,000 stars, with a further 60,000 stars assembled from a variety of pre-existing sources. As a result, the kinematics of stars used to construct the relationship between mean stellar age and the components of the velocity dispersion (the Age-Velocity relation, AVR) have been greatly improved. We briefly review here the state of the observational AVR both pre-Hipparcos and post-Hipparcos.

2.1 Observational Age-Velocity-Relation

Figure 1(a), shows several determinations of the AVR from the literature. We divide the measurements into pre-Hipparcos and post-Hipparcos determinations.

Each AVR presented and the simulation results has been fit with the following form

$$\sigma(t) = \sigma_o \left(1 + \frac{t}{\tau}\right)^\alpha \quad (1)$$

where $\sigma(t)$ is the total velocity dispersion as a function of time, t , σ_o is the initial velocity dispersion at $t = 0$, τ is a constant with unit of time, and α is the heating index (Wielen 1977; Villumsen 1985). Our motivation here is to fit the data with a simple analytical law which can also be fit to the simulations.

2.1.1 Pre-Hipparcos determinations

Firstly, consider the pre-Hipparcos measurements of the AVR, which are shown in panel a_1 of Figure 1. Edvardsson et al's (1993) data set of accurately determined ages for 189 F and G stars is shown by crosses. Wielen's (1977) determination, based mainly on K and M dwarfs which have been ranked by age based on chromospheric emission line measurements, is shown by squares. An improved version of the data set (Fuchs & al. 2000) is shown by triangles. These latter data sets are mostly M dwarf types, for which the kinematical and parallax measurements have only been marginally improved by Hipparcos, and they remain robust in the post-Hipparcos epoch.

We have fit each data set to Eqn 1, using a non-linear least squares gradient-expansion algorithm (using the IDL software package). All data points were given equal weight. For these three data sets, we find heating indices α in the range 0.47 to 0.61 (see Table 1).

Our motivation is to fit the same form of the heating law to all the available data and to all the simulations. We should note that the heating indices α we derive are not quite the same as those derived by the authors above, who apply additional physical constraints to the fitting (e.g. the nature of the stellar orbital diffusion, and the weight to be applied to the initial value of the velocity dispersion). Nevertheless, the fitted indices are similar.

2.1.2 Post-Hipparcos determinations

We now consider post-Hipparcos AVR determinations (Figure 1(a_2)). Circles show data from Holmberg (2001), for 1486

Table 1. Values of the heating index obtained by fitting data in the literature. The first five rows show our fits, and the last two show the author's own reported values. Note that Holmberg (2001) removes the effect of higher velocity thick disc stars when making his (more reliable) estimate of the heating index, whereas we leave them in (in order to estimate the bias they impose). There is a very considerable range in the derived values of α , which far exceeds the reported (internal) error estimates; α is therefore very likely to be dominated by systematic errors in the methods used to estimate stellar ages.

Study	α
R. Wielen (1977)	0.61 ± 0.04
Fuchs et al. (2000)	0.59 ± 0.04
Edvardsson et al.(1993)	0.47 ± 0.002
H. Rocha-Pinto	0.26 ± 0.008
Holmberg (2001) All stars	0.45 ± 0.04
Holmberg (2001) Thick Disc removed	0.33 ± 0.03
Binney et al. (2000)	0.33 ± 0.03

Hipparcos F and G type stars for which ages can be determined with an accuracy of about 30% (of the age), by fitting absolute magnitude and colours to stellar isochrones. We show by diamonds our analysis of data kindly provided in advance of publication by H. Rocha-Pinto, who has determined ages of 425 mainly F, G and K stars using a carefully calibrated technique based on chromospheric emission (Rocha-Pinto & Maciel 1998). For his stars we have measured the total velocity dispersion as a function of age for the objects with $[\text{Fe}/\text{H}] > -0.5$, being careful to exclude several high velocity outliers.

When fitting the data from H. Rocha-Pinto we yield a heating index $\alpha = 0.26$ with a very small (formal) error (see Table 1). However, the value of the heating index is sensitive to the fitting procedure. For example, if we had used bins of 60 stars instead of 40-star-bins, we would have obtained $\alpha = 0.29 \pm 0.02$. Because most of the stars in the sample were young we binned the data so that there were equal number of stars in each bin rather than using bins of equal width in age.

The data from Holmberg was fitted in similar manner: the objects with $[\text{Fe}/\text{H}] < -0.5$ were removed from the data set and equal number bin were used. We obtained $\alpha = 0.45 \pm 0.04$ for the heating index. This is close to Holmberg's own results ($\alpha = 0.46 \pm 0.02$) for all his stars. However, Holmberg extends his fitting procedure by separating the stellar data into thin and thick disc components by a maximum likelihood method, deriving a best fitting AVR for the thin disc for which the heating index is $\alpha = 0.33 \pm 0.03$.

Binney et al. (2000) have used a different approach to constrain the star forming history and velocity dispersion evolution in the Solar neighbourhood. They have used photometrically complete sample of 11,865 Hipparcos stars. By combining local colour-magnitude diagram with the Padua isochrones and, crucially, kinematic information, they have obtained a heating index of $\alpha = 0.33 \pm 0.03$ and a disc age of 11.1 ± 0.8 Gyr. The value obtained is consistent with Holmberg's, for a smaller set of stars drawn from the same source (Holmberg works with individually determined stellar ages, and limits himself only to those for which the age can be determined quite accurately).

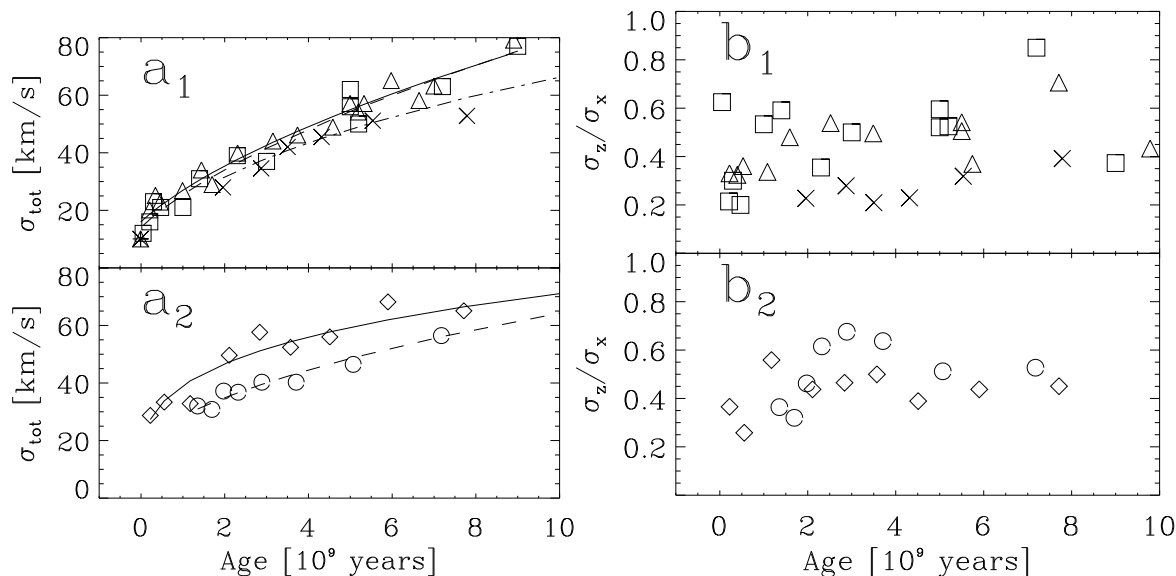


Figure 1. The observed total stellar velocity dispersion and ratio of velocity dispersions for nearby disc stars, as obtained by different authors. Best fits to the heating laws as parameterised by Eqn. 1 are also shown. Panel (a_1): the solid line is the fit to Fuchs et al. data (triangles), the dashed line is the fit to Wielen’s data (squares), and the dot-dashed line is the fit to Edvardsson et al. data (crosses). Panel (a_2): the solid line is the fit to Rocha-Pinto’s data (diamonds) and the dashed line is the fit to Holmberg’s data (circles). Panels (b_1) and (b_2) show the observed ratios of the vertical to the radial velocity dispersion for the same data sets and using the same symbols.

While the values of α obtained by Binney et al. (2000) and Holmberg (2001) are consistent, they are inconsistent with the value we derive from Rocha-Pinto’s data set, which uses an independent method to estimate stellar age, and inconsistent with the heating index derived for the K and M dwarfs, which have been age ranked via chromospheric emission (Fuchs & al. 2000). Fuchs et al. (2000) show that the discrepancy between values for the heating index of 0.3 and 0.5 is actually rather mild (see their Fig. 1), when plotted in the age-velocity dispersion plane.

The data sets give significantly different values for the heating index, ranging from 0.3 to 0.5. The error in the ages does give rise to a small systematic error in α ; we have performed Monte-Carlo simulations in which we change the ages of the observed stars by a Gaussian distributed random fractional error, and recomputed the fit for α . Random age errors of order 20% typically increase α slightly, typically by less than 0.05. A 20% error in stellar ages is realistic in the context of determining the heating index in the AVR. For example, Holmberg uses only stars with a fractional error of typically 20-30% (and always less than 50%), while Rocha-Pinto (private communication) reports fractional errors of order 30%. However, for the youngest stars in the sample, the errors may be significantly larger, of order 0.5 in $\log(\text{age})$. Monte-Carlo simulations show that this is certainly enough to reduce the heating index from 0.5 to 0.3. Furthermore, the determination of α is sensitive to systematic errors in the ages of the younger stars. We have performed Monte-Carlo simulations which show that changes in the value of α of order 0.1 can be obtained if, for example, there is a systematic error of 50% in the assigned ages of stars younger than a few Gyr (as might occur as a result of systematic errors in isochrone colours). There are thus

several mechanisms which could produce systematic errors in the heating index as derived from observations.

We are reluctant to arbitrarily assign any of these data sets greater credence than any other; they are all very carefully constructed and they use different techniques, some independent, to assign ages to the stars. Instead we move on to consider the ratio of the velocity dispersions, rather than the vertical velocity dispersion alone. This quantity turns out to be much less sensitive to the ages of the stars and turns out to be very useful in comparing the data to the simulations.

2.2 Ratio of Velocity Dispersions

In panels (b_1) and (b_2) of Figure 1 the ratio of the vertical to the radial velocity dispersion σ_z/σ_x is plotted for the same cases as in panels (a_1) and (a_2) and using the same symbols. The scatter seems to be larger amongst the pre-Hipparcos observations (panel (b_1)) than in the post-Hipparcos data (panel (b_2)). The latter observations indicate that the ratio is $\sigma_z/\sigma_x \simeq 0.5$ and the former observations corroborate this. Using the Hipparcos data, Dehnen and Binney (1998) have determined the velocity dispersion evolution as a function of colour index $B - V$. Their results also indicate that the ratio σ_z/σ_x tends to ~ 0.5 .

2.3 Comparing observations and simulations

The observations show that the heating index lies between $\alpha = 0.3$ and 0.5: in other words α is not yet well constrained by the observations. This was a major uncertainty in comparing the results of the simulations and observations. On the other hand, the ratio σ_z/σ_x is quite well measured at 0.5 ± 0.1 . The ratio of vertical velocity dispersion to radial

velocity dispersion thus turned out to be the best discriminator when theoretical models or numerical simulation are compared with observations (Sections 4, 5, and 6).

3 SIMULATION METHOD

The local simulation method was first used in planetary ring dynamics by Wisdom and Tremaine (1988) (see also Salo 1995) and was first applied to disc galaxies by Toomre (1990). In the method all calculations are restricted to a small co-moving box within the Galactic disc. A typical computer run simulates a “patch” of the disc, being 1×1 or 2×2 kpc square, and 2 to 4 kpc in vertical extent, containing of order 10^4 tracer stars in the disc as well as any perturbers (GMCs or BHs).

The coordinates of stars in the region are referred to a point which moves on a circular orbit around the Galactic center at a distance r . A rotating Cartesian coordinate system is placed at the reference position, the x -axis pointing radially outward (away from the Galactic center), the y -axis in the direction of orbital motion, and the z -axis in the direction normal to the Galactic plane. The orbits of stars in the patch are computed by integrating the linearized equations of motion (Hill 1878; Julian & Toomre 1966):

$$\begin{aligned} \ddot{x} - 2\Omega\dot{y} + (\kappa^2 - 4\Omega^2)x &= F_x \\ \ddot{y} + 2\Omega\dot{x} &= F_y \\ \ddot{z} + \nu^2 z &= F_z \end{aligned} \quad (2)$$

where Ω is the orbital frequency, and κ and ν are the epicyclic frequency and the vertical frequency of motion, respectively. The numerical integrator is the RK4 routine (Press & al. 1992). We adopt Solar neighbourhood ($r = 8$ kpc) values of $\Omega = 25.9 \text{ km s}^{-1} / \text{kpc}$, $\kappa = 36.0 \text{ km s}^{-1} / \text{kpc}$, and $\nu = 98.7 \text{ km s}^{-1} / \text{kpc}$ (Binney & Tremaine 1987). The tracer stars feel the Galactic potential and the forces due to perturbers (GMCs or black holes). In order to avoid numerical artefacts, the gravitational forces (F_x, F_y, F_z) are calculated so that Newton’s third law is satisfied, i.e. a perturber also feels the gravitational force from tracer stars.

3.1 Numerical accuracy

All the calculations are performed in double precision. In an unperturbed test run with an integration step size $\Delta t = T_{orb}/800$ the relative error in the stellar vertical kinetic energy was observed to be $|\Delta E_z/E_z(0)| < 4 \times 10^{-7}$ at the end of the simulation run ($t_{END} = 50T_{orb} \simeq 12 \text{ Gyr}$). Here $T_{orb} \simeq 237.23 \times 10^6$ years, is the orbital time around the Galactic center. During the run the vertical component of the system angular momentum relative to the reference position should remain zero, and is conserved to better than $|\Delta I_z|/\sqrt{I_z^2(0)} < 3 \times 10^{-14}$ in which we have compared the change in the system angular momentum to the mean initial angular momentum of the stars.

In the production runs we have used a still shorter integration step size: from $\Delta t = T_{orb}/1000$ to $\Delta t = T_{orb}/16000$ depending on the size and mass of the perturber. We have used such a short time step because the numerical accuracy of the orbits is dominated by the close encounters with the

massive perturbers. Most of the numerical error is due to these instances. The time step would be even shorter if we were interested in the orbits, but it is actually the statistical heating of many orbits which concerns us, rather than maximum accuracy for particular orbits. The time step was determined by simply testing how a shorter and shorter time step affects the evolution of the velocity dispersion. Because the integration error creates artificial noise in the system, we just need to search for the largest step size for which the velocity dispersion of the tracer stars does not increase due to step size in a simulation with massive perturbers. The optimal step size will naturally be different for a point mass like black holes and for an extended object like a GMC.

An important potential source for systematic error is in the calculation of gravitational force. In practice, because we are using a local simulation box, the calculation of the gravitational interaction has to be cut off at some distance. Furthermore, in a local simulation method this limit should be at most half of the box size, in order to avoid computing the gravitational force from a perturber more than once. We need to choose a box size for which the heating of the orbits by distant encounters outside the cut-off-radius is insignificant compared to closer encounters within the cut-off-radius. We have performed sets of simulations in order to test for the appropriate patch size. Some examples will illustrate this: for a $1 \times 1 \text{ kpc}^2$ patch and black holes with $M_{BH} = 1 \times 10^6 M_\odot$ we find the total stellar velocity dispersion after 50 Solar orbital periods rises to $\sigma_{tot} = 22.7 \text{ km s}^{-1}$; changing to a patch of $2 \times 2 \text{ kpc}^2$, and running the simulation again with a larger cutoff length for gravity, we derive a total velocity dispersion of 22.1 km s^{-1} at the end of the run. The difference between the runs is within the simulation noise level and we conclude that the effects of long range forces are simulated with good accuracy. For GMCs of similar mass the patch size $1 \times 1 \text{ kpc}^2$ was observed to be too small, and minimum size $2 \times 2 \text{ kpc}^2$ had to be used.

3.2 Boundary conditions and the tracer stars

Tracer stars move on epicycles in the patch, and can potentially cross the patch’s boundaries. Periodic boundary conditions are used to recover these stars, which enter from the opposite boundary with a correction made for Galactic shear, as described in detail by Wisdom and Tremaine (1988). The box in which the calculations are performed is thus effectively surrounded by virtual boxes which shear due to Galactic rotation, as illustrated in Figure 2. We typically use boxes which are $1 \times 1 \text{ kpc}$ or $2 \times 2 \text{ kpc}$ in the Galactic plane, and extend 2 or 4 kpc above and below it.

The linearized equations are valid as long as $|x|$ and $|z| \ll r$. For all our simulations the velocity dispersions remain low and this condition is met.

3.3 Massive Perturbers

We simulate two types of massive perturber: Giant Molecular Clouds (GMCs) and Black Holes (BHs). The GMCs are placed in the Galactic plane on near-circular orbits, which are then integrated in the same manner as the tracer stars (but without the effect of the other perturbers, as this would unnecessarily slow the simulation and heat up the GMC

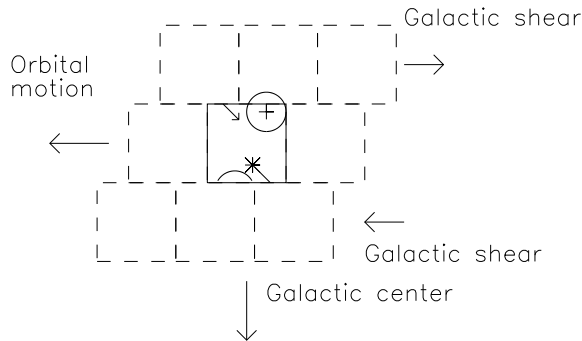


Figure 2. The simulation box (solid line) and its surrounding virtual boxes (dashed lines) are illustrated. Gravitational forces on a given star (cross) are calculated from the gravitational perturbers whose nearest image lies within the distance R_g (denoted by the circle). If a star (asterisk) leaves the simulation cell, its image will enter the cell in a way defined by the boundary conditions.

population). The same periodic boundary conditions which replaces those stars which leave the box are also applied to the GMCs.

The BHs are on orbits characteristic of the dark halo, with high velocities relative to the disc stars. BHs move through the box on essentially straight line orbits. They obey the same periodic boundary conditions as the tracer stars in the radial (x -) and azimuthal (y -) direction, but not in the vertical (z -) direction. The border in the z -direction is given special status, by setting it to be far enough from the disc midplane, in order that no forces need to be calculated across it. In practice one must take care that the box is large enough in the vertical direction, so that the stars never get close to the vertical boundary. When a halo black hole goes through the vertical border, it is removed from the simulation and a new one is randomly created from the parent velocity and space distribution. The number density of dark halo BHs entering and leaving the box is maintained at a constant level.

The orbits of the tracer stars are computed by solving Equation 2 in the presence of massive perturbers in the disc or moving through the disc from the Galactic halo, by direct summation. The forces are calculated on each tracer star for all perturbers which are within a radius R_g of the star (see Fig. 2). In practice we have always used the maximum distance allowed by the patch, *i.e.* the calculation radius is half of the box width.

4 DISC HEATING BY GIANT MOLECULAR CLOUDS

A number of studies of disc heating via GMCs have been made, either via numerical simulations or via more theoretical approaches, *e.g.* by numerically integrating the Fokker-Planck equation. Our aim here is to compare our simulation results with previous work, and to compare with the post-Hipparcos observations of the AVR.

Observations of the gas and dust in GMCs reveal a complex, fragmented structure that is often described as self-similar or fractal. We model our simulation GMCs by spherical mass distributions of uniform density. In many works (Villumsen 1983; Villumsen 1985) the GMCs have

been simulated as having a softened point potential (*e.g.* the Plummer model). However, when taking into account the complex structure of GMCs we have preferred using an homogeneous density distribution; we have thus modelled our GMCs as homogeneous spheres. The disc heating is not very sensitive to these differences in the modelling.

Because most of the mass of interstellar matter is in the high end of the molecular cloud mass function, it is sufficient to simulate only the most massive GMCs, having typical masses of $M_{\text{GMC}} = 1 \times 10^6 M_{\odot}$ and diameters of $d_{\text{GMC}} = 100 \text{ pc}$ (Scoville & Sanders 1986). Because GMCs do not interact with each other, the velocity dispersion of the GMC population is frozen during the simulation run. The observed velocity dispersion of the Galactic GMC population is so low that there must be some kind of physical mechanism for cooling it. There is some evidence that infalling gas into the Galactic disc cools down the interstellar gas. Whatever the physical mechanism, we can emulate this situation simply by allowing no interactions between the GMCs.

We start the simulations with both the tracer stars and the GMCs having a low (cold) velocity dispersion, simulating that the stars have just been born from the gas clouds, and share their kinematics. The values used are taken from Dehnen & Binney (1998). The total velocity dispersion σ is decomposed into three components in the x, y, z directions of $(\sigma_x, \sigma_y, \sigma_z)$, with $\sigma_x = 14 \text{ km s}^{-1}$ and $\sigma_z = 6 \text{ km s}^{-1}$ (σ_y follows from the σ_x and Ω/k -ratio). The initial velocity distribution is Gaussian. The initial vertical structure is Gaussian. Strictly speaking the vertical structure should obey a sech^2 -distribution in order to be isothermal, but in practice the sech^2 -distribution is very close to a Gaussian distribution in numerical simulations with a limited number of particles.

In the GMC runs the simulation box size $2 \times 2 \times 4 \text{ kpc}^3$ was found to be large enough for the calculation of gravitational perturbations. After testing it was found that an integration step size $\Delta t = T_{\text{orb}}/1000$ is sufficiently small for these runs, where $T_{\text{orb}} \simeq 237.23 \times 10^6$ years. At the Solar radius the radial distribution of molecular clouds is falling off rapidly with increasing radius. In the vicinity of the Solar neighbourhood the average density of molecular clouds is approximately $\Sigma_{\text{GMC}} \simeq 5 M_{\odot}/\text{pc}^2 = 5 \times 10^6 M_{\odot}/\text{kpc}^2$ (Scoville & Sanders 1986).

The evolution of the stellar velocity dispersion is plotted in Figure 3(a) for four different assumed GMC number densities in the patch: $\Sigma_{\text{GMC}} = 2, 4, 8, 16/\text{kpc}^2$. As most of the mass is at the high-mass end of the spectrum, the case $\Sigma_{\text{GMC}} = 4/\text{kpc}^2$ is closest to the present value for the Solar neighbourhood.

We have fit the simulations with an age-velocity relation (AVR) of the form given in Eqn 1. The second curve, from bottom to top, in Figure 3(a) shows the fit with the most appropriate values for the Solar neighbourhood. The velocity dispersion is fitted only for the values $\sigma_{\text{tot}} > 30 \text{ km s}^{-1}$, because the stellar heating by GMCs is known to obey a different power law when the stellar scale height is less than cloud scale height (Lacey 1984). Our fits are thus valid when the stellar population has a larger scale height than the GMC population. The velocity dispersion in the simulations is observed to grow as $\sigma(t) \propto t^{0.21}$ (see Table 2). This is slightly less than found in other studies ($\sigma(t) \propto t^{0.25}$ using different methods; *i.e.* analytical treatment in Lacey (1984), and

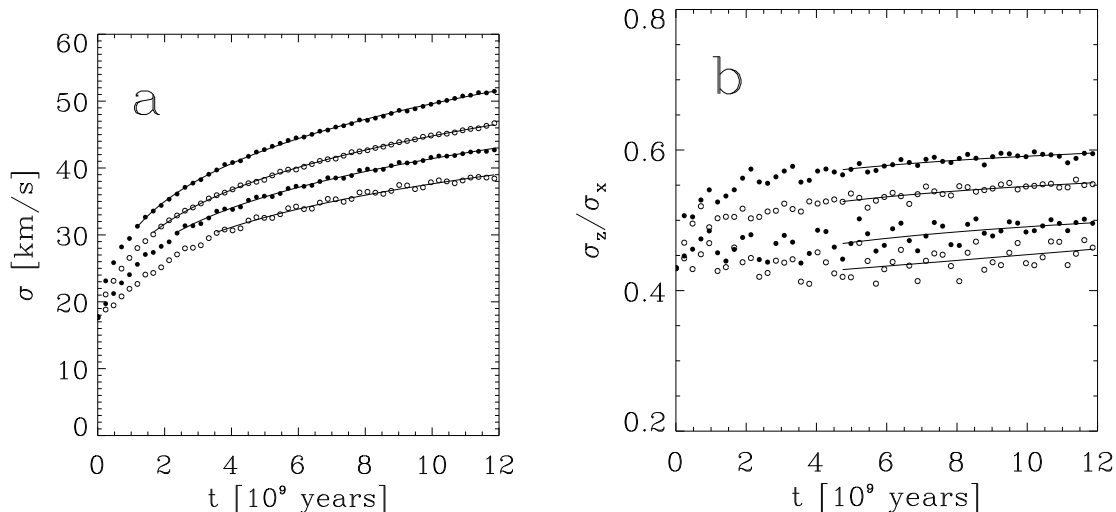


Figure 3. Panel (a). The evolution of total velocity dispersion σ due to GMCs. Symbols are the simulation results and the curves represent least squares fits of the Eq. 1 to the points. Panel (b): The ratio of the vertical to the radial velocity dispersion shown as a function of the number density of GMCs, Σ_{GMC} , in the simulation box. In both panels, from bottom to top, $\Sigma_{\text{GMC}} = 2, 4, 8, 16 \text{ kpc}^{-2}$.

“scaled” disc simulations in Villumsen (1985)). The least-square-fit-values for α are shown in Table 4 individually for the total σ_{tot} , the radial σ_x and the vertical component σ_z of the velocity dispersion. The vertical velocity dispersion is observed to grow more efficiently than the velocity dispersion in the horizontal plane. This tendency is in accordance with the earlier results (Villumsen 1985), but our values for the α are somewhat smaller.

The ratio σ_z/σ_x of the vertical velocity dispersion to the radial velocity dispersion is plotted in a Figure 3(b). The ratio is clearly a function of the number density of the GMCs. At the end of the simulation this ratio varies between about 0.45 and 0.60; i.e. the vertical heating is relatively most effective when the GMC number density is highest. However, all the values fall within the observational limits $\sigma_z/\sigma_x \simeq 0.5 \pm 0.1$. Coincidentally the mean value $\sigma_z/\sigma_x \simeq 0.5$ is produced by the case $\Sigma_{\text{GMC}} = 4/\text{kpc}^2$ which is approximately the present GMC (of mass $M_{\text{GMC}} = 1 \times 10^6 M_{\odot}$) number density in the Solar neighbourhood.

The ratio of the azimuthal component to the radial component depends on Ω and κ and is $\sigma_y/\sigma_x \simeq 0.7$ for the Solar neighbourhood. This is also what is observed in the simulations.

Our results seem to be in poor accordance with Lacey’s (1984) results; he predicts $\sigma_z/\sigma_x \simeq 0.8$ for the present values of the epicyclic constants. He has also obtained $\sigma \propto t^{0.25}$ for all the velocity components when the stellar scale height is larger than the GMC scale height.

Lacey generalized the work of Spitzer and Schwarzschild (1951; 1953) (who calculated the evolution of the stellar velocity distribution function by numerically integrating the Fokker-Planck equation) and calculated the evolution of all three components of the velocity dispersion by solving the first moments of the Fokker-Planck equation. He assumed that the velocity distribution always remains a triaxial Gaussian. Most importantly, the stellar orbits are as-

sumed to be predominantly perturbed by many distant, weak encounters so that the evolution of the distribution function could be described by the diffusion equation.

Lacey uses first-order epicyclic theory for the stellar orbits (as we do here) and assumes the molecular clouds to be long lived (as here). However, for simplicity he adopts circular GMC orbits, ignores Galactic shear and assumes that the interaction time between the stars and the GMCs is short.

A simple test is to vary the GMC size: a simulation run with $\Sigma_{\text{GMC}} = 4/\text{kpc}^2$ and $d_{\text{GMC}} = 20 \text{ pc}$ (which is similar to Lacey’s cloud size) yielded $\alpha = 0.23$ for the total velocity dispersion. This goes in the expected direction as smaller cloud size will increase the strength of the gravitational perturbation in the close encounters. We also find that the vertical component of the velocity dispersion is increased relative to the radial one; we observed $\sigma_z/\sigma_x \simeq 0.57$ at the end of the simulation. This partly explains the difference in the results. The remainder we ascribe to the assumptions in the analytical method (i.e. circular GMC orbits, no Galactic shear and short star-GMC interactions).

Numerical simulations by Villumsen (1985; 1983) have yielded $\sigma_z/\sigma_x \simeq 0.6$. He obtained similar results for the growth of the velocity dispersion in the plane as Lacey (1984). On the other hand, for the vertical velocity dispersion Villumsen obtained $\sigma_z \propto t^{0.31}$, which is significantly larger than the value we obtained ($\alpha = 0.26$).

Unfortunately, comparison of our results with Villumsen’s work is not straightforward because he analyses what one might term “scaled-up” simulations. Specifically, in his model, the exponential Galactic disc, with scale length 1.75 kpc, contains 4000 GMCs with total mass $M_{\text{tot}} = 4 \times 10^9 M_{\odot}$ outside 3 kpc radius, the individual GMCs having mass of $M_{\text{GMC}} = 1 \times 10^6 M_{\odot}$. This model is then scaled so that it could be simulated with fewer and heavier GMCs: the scaling being based on theoretical expectations (e.g. Lacey 1984) that in the diffusion process the efficiency is

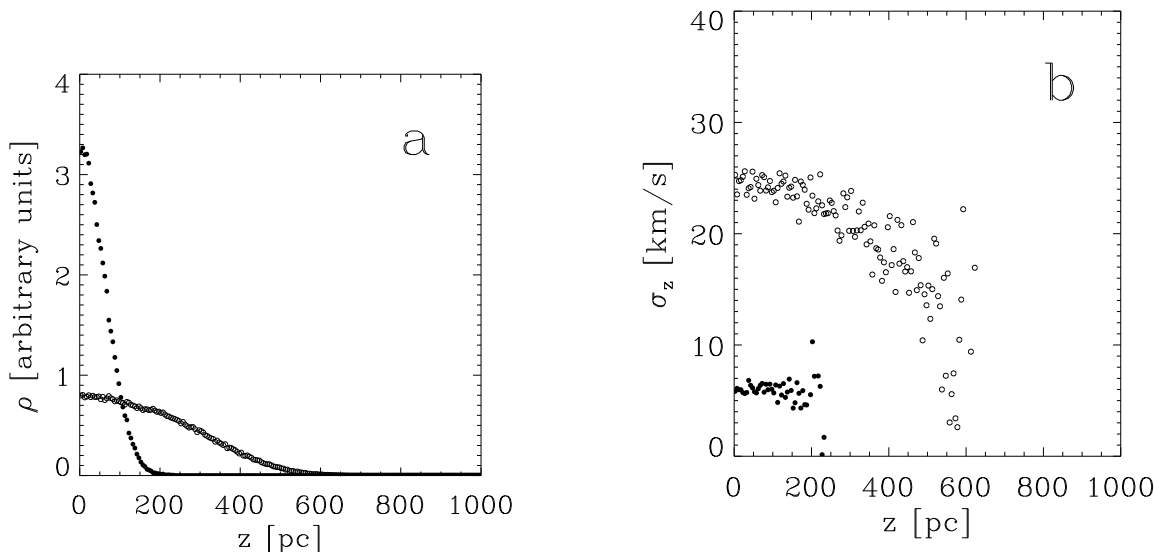


Figure 4. Panel (a): the vertical density profile of the stellar disc at the start (filled circles) and at the end (open circles) of the simulation for a GMC number density of $\Sigma_{\text{GMC}} = 16/\text{kpc}^2$. Panel (b): the vertical component of the velocity dispersion as a function of vertical height at the beginning (filled circles) and in the end (open circles) of the corresponding simulation.

proportional to the total number of GMCs (N_{GMC}) and to the square of the mass (M_{GMC}^2) of a single GMC, *i.e.* $N_{\text{GMC}} \times M_{\text{GMC}}^2 = \text{constant}$. In the actual simulations 200 or 400 GMCs with mass $M_{\text{GMC}} = 3.2 \times 10^6 M_{\odot}$ have been used. The GMC size is the same as ours ($d_{\text{GMC}} = 100 \text{ pc}$), but a Plummer model has been used for the GMC potential and the cut-off radius for the gravitational interaction has been set at 2 kpc. The numerical scheme is rather different from ours, but the equations of motion are integrated with a fourth order Runge-Kutta scheme as in our simulations. Villumsen utilised an integration step size $\Delta t = 3 \times 10^6$ years, corresponding to $\Delta t = T_{\text{orb}}/74$ at the Solar radius. In light of these many differences it is not surprising how difficult it is to compare our simulations with Villumsen’s.

One noticeable difference is, though, in the integration step size. Villumsen (1985) reported that relative numerical error in energy was less than 0.01% in an unperturbed simulation. However, the errors in the numerical orbit integration will be worst in close encounters between stars and massive GMCs. Based on our experience with our numerical scheme, a considerably larger step size than the one adopted by us induces artificial heating in the system.

The vertical density distributions of the tracer stars are plotted in Figure 4(a) both at the beginning and the end of the simulation run with $\Sigma_{\text{GMC}} = 16/\text{kpc}^2$. The initial density distribution (filled circles) is exactly Gaussian with scale height of $z_0 = 61 \text{ pc}$. At the end of the simulation run the vertical structure of the disc (open circles) is still almost Gaussian with an obviously much larger scale height ($z_0 \approx 230 \text{ pc}$). Compared to a Gaussian distribution the high end tail is missing and the central density maximum is slightly suppressed, *i.e.* the profile is more ‘boxy’, but still very close to a Gaussian.

The vertical velocity dispersion as a function of height is examined in Figure 4(b) for the same simulation. The initial velocity dispersion is isothermal (filled circles). At the end

Table 2. Fitting of the GMC heating. The least-square-fit of the exponent α of the Eq. 1 is tabulated for the simulation runs along with the number density of GMCs.

Σ [$1/\text{kpc}^2$]	α for σ_{tot}	α for σ_x	α for σ_z
2	0.207 ± 0.014	0.198 ± 0.019	0.263 ± 0.042
4	0.215 ± 0.010	0.208 ± 0.015	0.265 ± 0.031
8	0.217 ± 0.008	0.212 ± 0.012	0.263 ± 0.024
16	0.217 ± 0.007	0.214 ± 0.012	0.252 ± 0.015
avg	0.21	0.21	0.26

of the simulation run, however, the velocity dispersion is observed to decrease as distance from the horizontal plane increases. Also numerical simulations by Jenkins (1992) have indicated that in the coeval disc the molecular cloud heating mechanism does not retain an isothermal velocity dispersion, but the velocity dispersion drops in higher altitudes as in our results. His simulations also yield similar results concerning the vertical density distribution: it is more ‘boxy’ than in the isothermal disc.

To summarise the GMC section: our results rule out GMCs as the primary source of disc heating, because the GMC number density required to heat the disc by the correct amount is many times the observed GMC density in the Solar neighbourhood (and our results indicate that GMC heating is even less effective than earlier thought, *i.e.* $\sigma \propto t^{0.21}$). However, contrary to the earlier results, our simulations indicate that the velocity ellipsoid is quite flat and consistent with the observational constraint on σ_z/σ_x .

5 HEATING DUE TO HALO BLACK HOLES

Another possibility for the heating of the Galactic disc would be due to gravitational interaction with massive black holes in the Galactic dark halo, which would make up part or all of the Galaxy's dark matter (Lacey & Ostriker 1985). These authors estimate that black holes of mass $M_{BH} \approx 2 \times 10^6 M_\odot$ orbiting inside the Galactic halo could explain the observed disc heating if they comprised the entire dark halo.

One should note that there are clear difficulties with the black hole scenario. Based on estimates of the accretion rate of gas onto black holes which are passing through the disc, (McDowell 1985) rule out more massive black holes than $M_{BH} = 1000 M_\odot$. Accretion should make such black holes directly observable as optical or infrared objects, but no such objects have been found. Lacey and Ostriker (1985) estimate that the accretion of the ISM onto the $M_{BH} \sim 10^6 M_\odot$ halo black holes would create a number of X-ray sources which should have been observed if they existed. On the other hand, recent work on the Galactic center black hole, which has a mass of $2.6 \times 10^6 M_\odot$ (Genzel 1998; Narayan & al. 1998), shows it to be a remarkably dim X-ray source despite the high density of gas in which it sits, which indicates that estimates of the X-ray flux of much nearer black holes of similar mass passing through the disc ISM may be overestimated by several magnitudes.

Furthermore, this scenario has also purely dynamical difficulties. Very massive black holes in the Galactic halo might also disrupt globular clusters in close encounters within the Hubble time. Moore (1993) estimates that the existence of the present population of low-mass globular clusters sets an upper limit of $M_{BH} = 10^3 - 10^4 M_\odot$ for the black hole masses. Klessen and Burkert (1996) estimate the upper limit to be $M_{BH} = 5 \times 10^4 M_\odot$. However, there are also some difficulties when deducing these upper limits. First of all, we do not know the initial mass function of globular clusters. Secondly, as the evolution of a globular cluster is mainly affected by BH encounters within its small core region and as these events are rare, only few events during a Hubble time determine its fate. There will be thus large statistical variations in globular cluster lifetimes.

Another limit on this scenario is introduced by the effects of dynamical friction. Lacey and Ostriker (1985) have estimated that black holes of mass $M_{BH} = 2 \times 10^6 M_\odot$ with initial orbital radii $r_{BH} < 2$ kpc would spiral into the Galactic center within $t = 15 \times 10^9$ years. They assumed circular orbits for the black holes. The actual value for the spiralling radius depends on the background density distribution which is still not accurately known.

Given these uncertainties, we attempt in this paper to establish constraints for the halo black hole population based purely on the kinematic evidence of heating in the Galactic disc, and ignore these other physical constraints.

We test here the black hole scenario by simulating a patch of the local disc embedded in a dark Galactic halo composed all or partly of massive black holes. The black holes have been treated as point masses. We have simulated two different mass objects: $M_{BH} = 1 \times 10^6 M_\odot$ and $M_{BH} = 1 \times 10^7 M_\odot$. We have chosen these masses because smaller masses have an insignificant effect, and bigger masses are difficult to simulate in the present method (*i.e.* using a patch — the patch should be made so large that one

would need to begin to take into account global properties of the Galaxy. In any case, black holes larger than $10^8 M_\odot$ can be ruled out because they would produce far too much heating, destroying the disc and/or destroying halo globular clusters (Carr 1994).

A softening of $\epsilon = 1$ pc has been used for the black holes in order to avoid numerical problems.

The black holes are assumed to have zero net rotation around the Galactic center and a 1-D Gaussian velocity dispersion of $\sigma_x = \sigma_y = \sigma_z = 135 \text{ km s}^{-1}$. Black holes pass through the simulation box with randomly chosen velocities drawn from these kinematics. The stellar population has the same initial velocity dispersion as in the GMC simulation runs.

5.1 $10^6 M_\odot$ Black Holes

In the runs with $M_{BH} = 1 \times 10^6 M_\odot$, the patch size was set at 1×1 kpc² in the horizontal plane. Different patch sizes were tested, but this size patch was found to be adequate. We have used 2 kpc for the vertical extent of the simulation box. The integration step size has to be small enough in order not to produce artificial heating. After some testing we found that $\Delta t = T_{orb}/8000$ is small enough.

We used 5000 stars in the patch and we investigated the effect of the number density of black holes on the disc heating. Figure 5(a) shows the evolution of the total velocity dispersion in five different cases: $\rho_{BH} = 4, 8, 16, 32, 64/\text{kpc}^3$. These number densities correspond to mass densities $\rho_{BH} = 0.004, 0.008, 0.016, 0.032, 0.064 M_\odot/\text{pc}^3$, respectively. For comparison, the mass density of the dark halo in the Solar neighbourhood is $\rho_H \sim 0.01 M_\odot/\text{pc}^3$ (Holmberg & Flynn 2000), so the two higher number density runs are clearly unrealistic, and their purpose is mainly to illustrate the effectiveness or non-effectiveness of this heating mechanism.

It is already clear from Figure 5(a) that in order to account for the amount of disc heating that is observed in the Solar neighbourhood there should be an unrealistically large number of $10^6 M_\odot$ black holes — the total mass of the black hole population would be larger than the mass of the whole Galactic halo.

We have again used Eq. 1 in the least-square-fitting of the velocity dispersion. The resulting exponent α for the total, radial, and vertical velocity dispersions can be seen in Table 3. Our simulations verify the results of Lacey & Ostriker (1985) that the total velocity dispersion is proportional to $\sigma \propto t^{0.5}$ for the heating due to the halo black holes.

They also found that the vertical-radial-axis-ratio is $\sigma_z/\sigma_x = 0.67$ in the non-selfgravitating case and $\sigma_z/\sigma_x = 0.55$ in the self-gravitating case. For $10^6 M_\odot$ black holes we find that σ_z/σ_x ranges from 0.47 to 0.67, the highest ratio being for the highest black hole density (see Fig. 5b). The lowest value for σ_z/σ_x -ratio is also closest to the observed value $\sigma_z/\sigma_x = 0.5 \pm 0.1$

The development of the vertical density profile in the simulation with $M_{BH} = 1 \times 10^6 M_\odot$ and $\rho = 32/\text{kpc}^3$ is shown in Figure 6(a). The density profile remains very close to a Gaussian, and has a half width of $z_0 \approx 350$ pc. The vertical component of the velocity dispersion is plotted in Figure 6(b) as a function of vertical distance from the horizontal plane. The velocities remain isothermal up to high

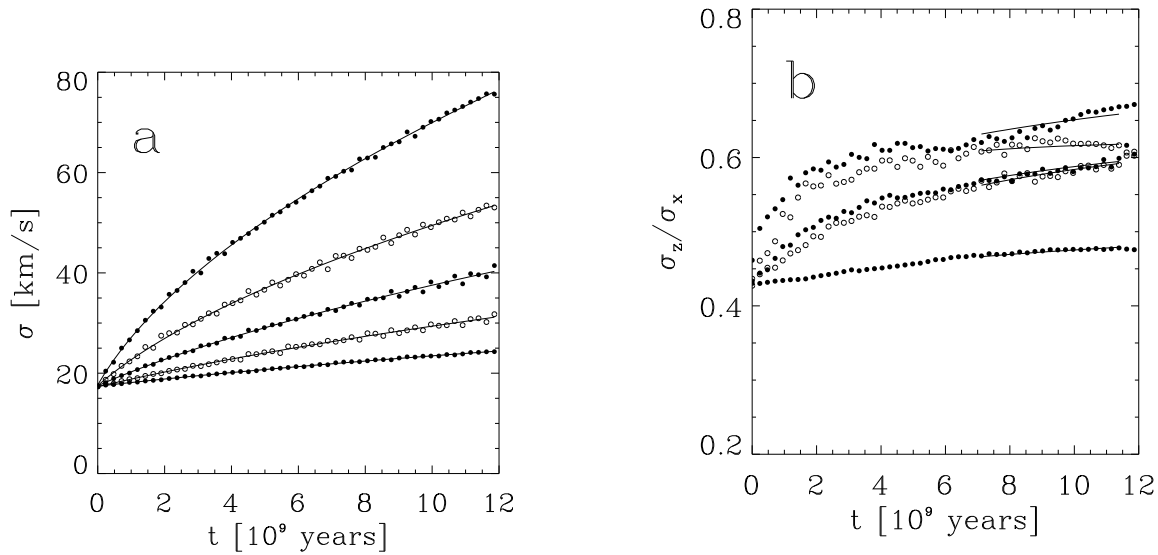


Figure 5. Panel (a): the evolution of velocity dispersion σ due to halo black holes of mass $M = 1 \times 10^6 M_\odot$. The curves represent simulation runs with black hole number densities $\rho_{BH} = 4, 8, 16, 32, 64/\text{kpc}^3$ from bottom to top. Panel (b): the evolution of the ratio of the vertical velocity dispersion to the radial velocity dispersion for the same simulations.

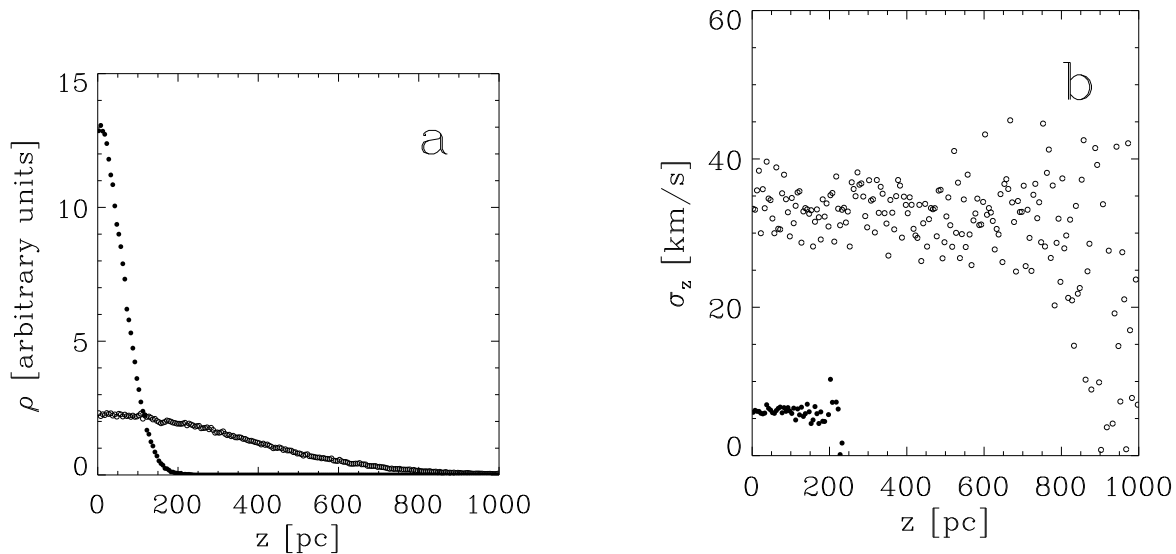


Figure 6. Panel (a): The vertical density profile of the stellar disc is plotted at the beginning and end of the simulation. Panel (b): the vertical component of the velocity dispersion of the stellar disc is plotted as a function of height at the beginning and end of the simulation. The adopted black hole mass is $M_{BH} = 1 \times 10^6 M_\odot$ and the number density is $\rho_{BH} = 32/\text{kpc}^3$.

altitudes, in this case up to about 700 pc at the end of the simulation.

5.2 $10^7 M_\odot$ Black Holes

For the $M_{BH} = 1 \times 10^7 M_\odot$ simulation runs a larger patch size was necessary. The used patch size was $2 \times 2 \text{kpc}^2$ in the horizontal plane and 4 kpc for the vertical size. The main reason for increasing the patch size is that we have to cal-

culate gravity from larger distances with the more massive perturbers.

The cutoff radius for calculating gravity was thus $R_g = 1 \text{kpc}$. Testing showed that a smaller integration step size was also needed, and we adopted $\Delta t = T_{orb}/16000$.

For these simulations, 10,000 stars were placed in the patch. We used black hole number densities of $\rho_{BH} = 0.25, 0.5, 1.0/\text{kpc}^3$, which correspond to mass densities $\rho_{BH} = 0.0025, 0.005, 0.01 M_\odot/\text{pc}^3$, respectively. The evolution of the total velocity dispersion is plotted in Figure

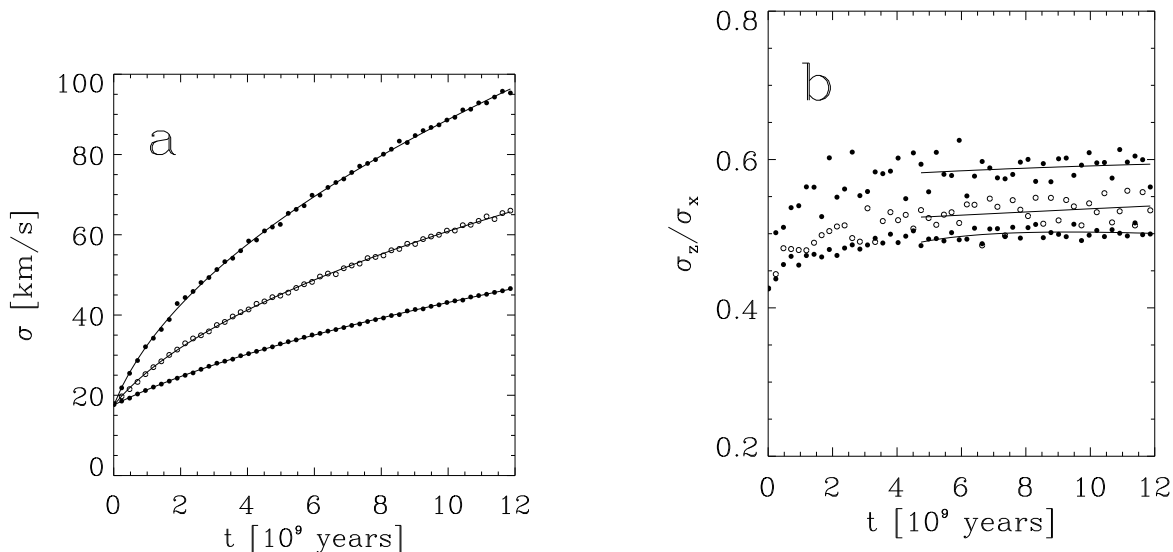


Figure 7. Panel (a): the evolution of velocity dispersion σ due to halo black holes of mass $M = 1 \times 10^7 M_\odot$. Panel (b): the evolution of the ratios of the vertical velocity dispersion to the radial velocity dispersion is plotted. The curves represent simulation runs with black hole number densities $\rho_{BH} = 0.25, 0.5, 1.0/\text{kpc}^3$ from bottom to top.

Table 3. Fitting of the disc heating index α due to the black holes of mass $M = 1 \times 10^6 M_\odot$.

ρ [$1/\text{kpc}^3$]	α for σ_{tot}	α for σ_x	α for σ_z
4	0.529 ± 0.014	0.507 ± 0.018	0.597 ± 0.030
8	0.514 ± 0.026	0.524 ± 0.040	0.498 ± 0.038
16	0.535 ± 0.057	0.522 ± 0.082	0.573 ± 0.098
32	0.53 ± 0.13	0.52 ± 0.19	0.56 ± 0.18
64	0.42 ± 0.29	0.42 ± 0.40	0.44 ± 0.51
avg	0.51	0.50	0.53

7(a). It is interesting to note that it would take about 8 billion years to heat up the stellar disc from $\sigma \simeq 18 \text{ km s}^{-1}$ to $\sigma \simeq 80 \text{ km s}^{-1}$ if the total mass of the halo consisted of $M_{BH} = 1 \times 10^7 M_\odot$ mass black holes. There are some ambiguity in the observations: some results indicate that the oldest stellar population would have a total velocity dispersion only of $\sigma \simeq 50 \text{ km s}^{-1}$. In this case the required amount of heating would be produced if only half the halo mass were in the form of these black holes. The RMS-fits of α for different components of the velocity dispersion are found in Table 4.

In addition to the fact that these black holes broadly produce the right amount of disc heating, they also distribute the heating in the three components consistently with observations. The σ_z/σ_x -ratios, plotted in a Figure 7(b), range from 0.5 to 0.6, the highest black hole number density producing highest σ_z/σ_x -ratio. Because of the ambiguity in the observed AVR, the massive halo black holes can not be ruled out as being responsible for the heating

Table 4. Fitting of the disc heating due to the black holes of mass $M = 1 \times 10^7 M_\odot$. Also the standard deviation for the fitted parameter is given as an error estimate.

ρ [$1/\text{kpc}^3$]	α for σ_{tot}	α for σ_x	α for σ_z
0.25	0.52 ± 0.04	0.53 ± 0.06	0.50 ± 0.04
0.5	0.48 ± 0.02	0.48 ± 0.02	0.50 ± 0.04
1.0	0.503 ± 0.008	0.502 ± 0.012	0.509 ± 0.016
avg	0.50	0.50	0.50

of the Galactic disc. However, if more weight is put on the post-Hipparcos AVR determinations, then the value $\alpha = 0.5$ could be considered being too high.

Our results are in mild disagreement with the theoretical expectations of Lacey and Ostriker (1985). They estimated that in order to heat the stellar disc from $\sigma \approx 10 \text{ km s}^{-1}$ up to $\sigma \approx 80 \text{ km s}^{-1}$ in 15 Gyr the halo ($\rho = 0.01 M_\odot/\text{pc}^3$) should be comprised of black holes of mass $M_{BH} = 2 \times 10^6 M_\odot$. Our simulations show that even $M_{BH} = 1 \times 10^7 M_\odot$ would not be enough to do the job. If the initial velocity dispersion were around $\sigma \simeq 10 \text{ km s}^{-1}$, the disc would be heated only to $\sigma \simeq 60 \text{ km s}^{-1}$ in 15 Gyr. (Note that Fig. 7(a) may be deceiving because a higher initial velocity dispersion, $\sigma \simeq 18 \text{ km s}^{-1}$, was adopted).

6 COMBINED EFFECT OF GMCS AND HALO OBJECTS

In order to test the combined effects of the GMCs and halo black holes on the disc heating we performed two further sets of simulations. We know approximately the number density of the giant molecular clouds in the Solar neighbourhood,

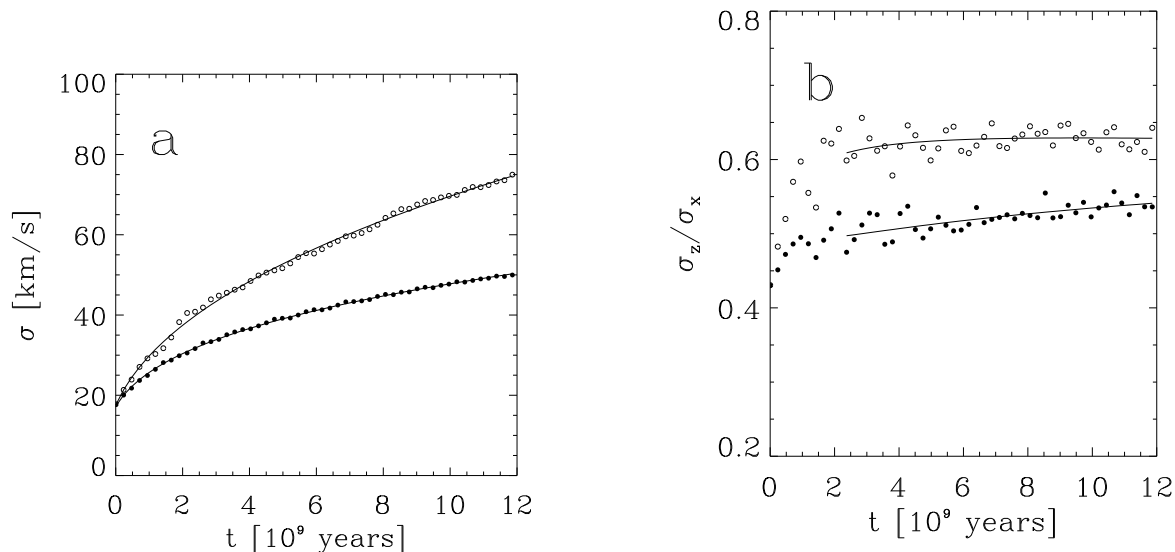


Figure 8. Panel (a): the total velocity dispersion of the stellar disc. The combined effect of the GMC and black hole perturbations are seen with two different masses of the halo black holes: $M_{BH} = 1 \times 10^6 M_{\odot}$ (filled circles) and $M_{BH} = 1 \times 10^7 M_{\odot}$ (open circles). Panel (b): the evolution of the ratios of the vertical velocity dispersion to the radial velocity dispersion.

but none of the parameters related to the possible black hole population are directly known, except for the local density of the dark halo.

The simulations seen in Figure 8 differ only by the number density and mass of the halo black holes. In the run of $M_{BH} = 1 \times 10^6 M_{\odot}$ the number density of the black holes is $\rho_{BH} = 8/\text{kpc}^3$ corresponding to $\rho_{BH} = 0.008 M_{\odot}/\text{pc}^3$. In this scenario most of the halo would thus consist of black holes. The combined effect of these black holes and GMCs would be enough to heat the disc to $\sigma = 50 \text{ km s}^{-1}$ in 12 Gyr (filled circles in Figure 8(a)), which is somewhat less than what is actually observed (however, see also Dehnen & Binney (1998) who report a maximum velocity dispersion $\sigma \simeq 50 \text{ km s}^{-1}$ for the oldest stellar population). The growth of the velocity dispersion is now intermediate between the pure black hole and the GMC cases alone, $\alpha = 0.31$.

The ratio of the vertical and radial components of the velocity dispersion is plotted in Figure 8(b). In this case (filled circles) the ratio is around $\sigma_z/\sigma_x \simeq 0.53$ after $t \simeq 10$ Gyr. This value fits well within observational error.

The open circles in Figure 8 show the simulation with halo black holes of mass $M_{BH} = 1 \times 10^7 M_{\odot}$, and a number density of $\rho_{BH} = 0.5/\text{kpc}^3$ which corresponds to $\rho_{BH} = 0.005 M_{\odot}/\text{pc}^3$. We can reproduce the disc heating very nicely with this setup, with the velocity dispersion rising to $\sigma \simeq 75 \text{ km s}^{-1}$ over 12 Gyr, very similar to the observations. The fitted heating law is within the observational limits at $\alpha = 0.42$. The ratio of σ_z/σ_x is about 0.63, which is also within the observational error limits.

It is interesting to note the high σ_z/σ_x ratios that the combined perturbations of BHs and GMCs produce. Why is the σ_z/σ_x ratio not somewhere between the values obtained from the simulations in which BHs and GMCs act alone? The answer lies in the fact that σ_z/σ_x ratio has a tendency to grow when the number of perturbers is increased, as seen in both the GMC and BH simulation sets. When we increase

the total number of perturbers, even if some of them are BHs and some GMCs, the σ_z/σ_x ratio is bound to increase.

7 CONCLUSIONS

There is firm observational evidence for the heating of the stellar disc with time. We have assembled the available post-Hipparcos samples of ages and kinematics for nearby stars and fit a heating law of the form $\sigma(t) = \sigma_0(1 + t/\tau)^\alpha$ to the data, where σ is the stellar velocity dispersion. The observational data limit α to values between about 0.3 and 0.6, i.e. despite the recent advances in measuring the kinematics and ages of nearby stars due to the availability of Hipparcos data, the age velocity relation in the nearby disc remains poorly determined. Fortunately, the ratio of the vertical component of the velocity dispersion to the radial component $\sigma_z/\sigma_x \simeq 0.5 \pm 0.1$ is much better constrained by available data and can be used to test our simulations.

We simulate disc heating by modelling a patch of the Galactic disc populated with tracer stars. We examine the effect of Giant Molecular Clouds (GMCs) travelling on disc orbits through the patch, and of massive black holes travelling through on plunging orbits characteristic of the dark halo.

In our simulations of GMC heating we consistently find slightly lower values for α than earlier studies have found, which are based on either theoretical estimates of the diffusion rate of stellar orbits, or scaled simulations of the whole Galactic disc (with a small number of GMCs). We find $\alpha = 0.21 \pm 0.02$ for the evolution of the total velocity dispersion and $\alpha = 0.26 \pm 0.04$ for the evolution of the vertical component of the velocity dispersion. The ratio σ_z/σ_x of heating in the vertical and horizontal directions in the disc is found to depend on the adopted GMC density.

The observed heating can not be explained by GMCs,

because even a four-fold GMC number density compared to the present day value in the Solar neighbourhood, $\Sigma \sim 5 M_{\odot}/\text{pc}^2$ (Scoville & Sanders 1986), does not heat up the disc enough. However, coincidentally we find that for the present day GMC number density the ratio $\sigma_z/\sigma_x \simeq 0.5$ which is consistent within the observational limits for stars in the local disc.

We have also run simulations of the local disc heating being caused by massive (10^6 - $10^7 M_{\odot}$) black holes of the dark halo penetrating the disc and perturbing the stellar orbits. Our simulations verify analytically obtained results in the literature, that the heating index is of order $\alpha = 0.5$. Even if the entire halo consisted of $M_{BH} = 1 \times 10^6 M_{\odot}$ black holes, the resulting heating of the stellar disc would be much less than what is observed. However, if the whole halo were comprised of black holes of order $M_{BH} = 1 \times 10^7 M_{\odot}$ the disc would be heated sufficiently. They would heat the disc in such a way that the ratio σ_z/σ_x would increase from 0.5 to 0.6 which is still within the error limits of the observations.

We have examined how the stellar disc would be heated by the combination of GMCs and halo black holes. Adopting a GMC density consistent with the present observed value and a dark halo comprised of $M_{BH} = 1 \times 10^6 M_{\odot}$ black holes would only heat the disc up to $\sigma \simeq 50 \text{ km s}^{-1}$ in 12 Gyr, which is inconsistent with most of the observations. On the other hand, if half of the halo were made of $M_{BH} = 1 \times 10^7 M_{\odot}$ black holes, they could with the GMCs heat the disc up to $\sigma \simeq 75 \text{ km s}^{-1}$ in 12 Gyr, which is consistent with observations, but the heating would also push the ratio of the vertical velocity dispersion to the horizontal dispersion higher: $\sigma_z/\sigma_x \simeq 0.63$, which is still barely within the observational limits. In this case the heating index was observed to be $\alpha = 0.42$.

Taking into account the observational uncertainties in the stellar disc heating we can produce the right amount of the heating by a proper combination of massive halo black holes, $M_{BH} = 1 \times 10^7 M_{\odot}$, and the right number density of GMCs in the Solar neighbourhood. Also the ratio σ_z/σ_x and the heating index α fall within observational error limits. We do not regard this as a particularly satisfactory solution, because there are other potential causes of heating of stellar orbits, such as spiral arms, which we plan to investigate further in the simulation method presented here.

ACKNOWLEDGMENTS

We are grateful to Burkhard Fuchs, Johan Holmberg, Heikki Salo, Jesper Sommer-Larsen, Alexandr Mylläri and Helio Rocha-Pinto for valuable discussions. We thank the Academy of Finland for supporting this work, through its support of the ANTARES space research program.

REFERENCES

Barbanis, B., Woltjer, L., 1967, ApJ, 150, 461
 Binney J., Dehnen, W., Bertelli, G., 2000, MNRAS, 318, 658
 Binney J., Tremaine S., 1987, Galactic Dynamics, Princeton University Press
 Carlberg, R., 1987, ApJ, 322, 59
 Carr, B., 1994, ARA&A, 32, 531
 Carr, B., Lacey, C., 1987, ApJ, 316, 23

Dehnen W., Binney J. J., 1998, MNRAS, 298, 387
 Edvardsson, B., Andersen, J., Gustafsson, B., Lambert, D., Nissen, P., Tomkin, J., 1993, A&A, 275, 101
 Friese, V., Fuchs, B., Wielen, R., 1995, in van der Kruit, P.C., Gilmore, G.F., eds., Proc. IAU Symp. 164, Stellar populations. Kluwer, Dordrecht, p. 414
 Fuchs, B., Dettbarn, C., Wielen, R., 1994, in Gurzadyan, V.G., Pfenniger, D., eds., Lecture Notes in Physics 430, Ergodic concepts in stellar dynamics. Springer-Verlag, Berlin, p. 34
 Fuchs, B., Dettbarn, C., Jahreiss, H., Wielen, R., 2000, astro-ph/0009059
 Genzel, R., 1998, Nature, 391, 17
 Hill, G., 1878, Am. J. Math., 1, 5
 Holmberg, J., Flynn, C., 2000, MNRAS, 313, 209
 Holmberg, J., 2001, A&A, submitted
 Jenkins, A., Binney, J., 1990, MNRAS, 245, 305
 Jenkins, A., 1992, MNRAS, 257, 620
 Julian, W., Toomre, A., 1966, ApJ, 146, 810
 Klessen, R., Burkert, A., 1996, MNRAS, 280, 735
 Lacey, C., 1984, MNRAS, 208, 687
 Lacey, C., Ostriker, J. 1985, AJ, 299, 633
 McDowell, J. 1985, MNRAS, 217, 77
 Moore, B., 1993, ApJ, 413, L93
 Moore, B., Ghigna, S., Governato, F., Lake, G., Quinn, T., Stadel, J., 1999, ApJ, 524, L19
 Narayan, R., Mahadevan, R., Grindlay, J., Popham, R., Gammie, C., 1998, ApJ., 492, 554
 Press, W., Teukolsky, S., Vetterling, W., Flannery, B. 1992, Numerical Recipes in FORTRAN, Cambridge University Press
 Rocha-Pinto, H. J., Maciel, W. J., 1998, MNRAS, 298, 332R
 Salo, H., 1995, Icarus, 117, 287
 Quinn, P., Hernquist, L., Fullager, D. 1993, ApJ, 403, 74
 Scoville, N., Sanders, D. 1986, in Smoluchowski et al., eds., The Galaxy and the Solar System. The University of Arizona Press, Tucson, p. 69
 Sommer-Larsen J., Flynn C., Christensen P. R., 1994, MNRAS, 271, 94.
 Spitzer, L., Schwarzschild, M., 1951, ApJ, 114, 385S
 Spitzer, L., Schwarzschild, M., 1953, ApJ, 118, 106S
 Toomre, A. 1990, in Wielen, R., ed, Dynamics and Interactions of Galaxies. Springer-Verlag, Berlin, p. 292
 Velazquez, H., White, S. 1999, MNRAS, 304, 254
 Villumsen, J. 1983, ApJ, 274, 632
 Villumsen, J. 1985, ApJ, 290, 75
 Wielen R., 1977, A&A, 60, 263
 Wisdom, J., Tremaine, S. 1988, AJ, 95, 925